

Partially Bio-Based Aromatic Polyimides Derived from 2,5-Furandicarboxylic Acid with High Thermal and Mechanical Properties

Kai Ma,^{1,2} Guofei Chen,¹ Wei Wang,¹ Anjiang Zhang,¹ Yingying Zhong,³ Yajie Zhang,¹ Xingzhong Fang ¹

¹Key Laboratory of Additive Manufacturing Materials of Zhejiang Province, Ningbo Institute of Material Technology and Engineering, Chinese Academy of Sciences, Ningbo, Zhejiang 315201, China

²University of Chinese Academy of Sciences, 19A Yuquan Rd., Shijingshan District, Beijing 100049, China

³Ningbo Entry-Exit Inspection and Quarantine Bureau Technology Center of the People's Republic of China, Ningbo, Zhejiang 315012, China

Correspondence to: G. Chen (E-mail: gfchen@nimte.ac.cn) or X. Fang (E-mail: fxzhong@nimte.ac.cn)

Received 4 December 2017; accepted 20 January 2018; published online 22 February 2018

DOI: 10.1002/pola.28982

ABSTRACT: Two novel bio-based diamines are synthesized through introduction of renewable 2,5-furandicarboxylic acid (2,5-FDCA), and the corresponding aromatic polyimides (PIs) are then prepared by these diamines with commercially available aromatic dianhydrides via two-step polycondensation. The partially bio-based PIs possess high glass transition temperatures (T_g s) in the range from 266 to 364 °C, high thermal stability of 5% weight loss temperatures ($T_{5\%}$ s) over 420 °C in nitrogen and outstanding mechanical properties with tensile strengths of 79–138 MPa, tensile moduli of 2.5–5.4 GPa, and elongations at break of 3.0–12.3%. Some colorless PI films (PI-

1-b and PI-1-c) with the transmittances at 450 nm over 85% are prepared. The overall properties of 2,5-FDCA-based PIs are comparable with petroleum-based PI derived from isophthalic acid, displaying the potential for development of innovative bio-based materials. © 2018 Wiley Periodicals, Inc. *J. Polym. Sci., Part A: Polym. Chem.* **2018**, *56*, 1058–1066

KEYWORDS: bio-based diamines; 2,5-furandicarboxylic acid; high performance polymers; polyimides; structure–property relations

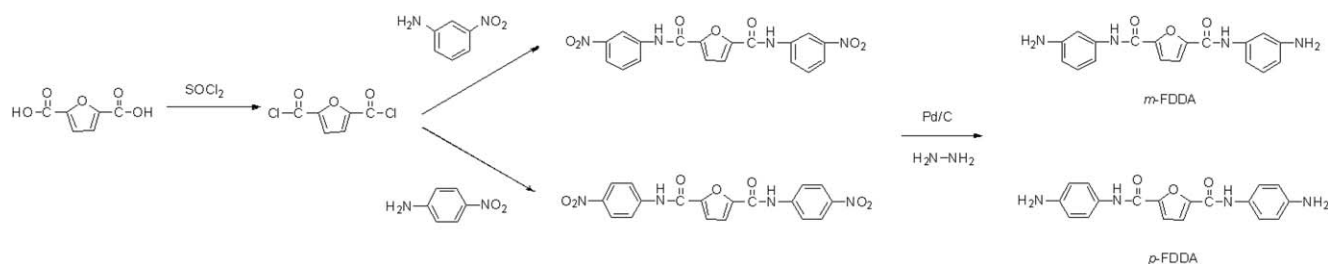
INTRODUCTION Over the recent years, a rapid development of renewable and bio-based polymers has advanced dramatically to suit emerging desire for sustainable development and the increasing concern about environmental pollution. However, these bio-based polymers are mainly aliphatic polymers, such as polyesters,^{1,2} polyurethanes,³ polycarbonates,⁴ poly(lactic acid),⁵ and polyhydroxyalkanoate,⁶ which mainly derived from cellulose,⁷ cardanol,⁸ vegetable oils,^{9,10} and lignins.¹¹ The poor thermal and mechanical properties of these polymers limited the application as high performance resins. Currently, an aromatic bio-based monomer, 2,5-furandicarboxylic acid (2,5-FDCA), which was mainly obtained through the catalytic conversion of biomass 5-hydroxymethylfurfural (HMF), has been increasingly used as precursor to form novel bio-based polymers. Nevertheless, the study of 2,5-FDCA-based polymers was mainly focused on polyester and polyamides with glass transition temperatures (T_g s) \leq 180 °C and melting temperatures (T_m s) \leq 215 °C.^{12–15}

Aromatic polyimides (PIs), considered as one of the most advanced classes of high performance polymeric materials,

have been intensively exploited in many applications such as optoelectronic devices,^{16,17} gas separation,¹⁸ smart materials,^{19,20} and composite materials,^{21,22} arising from their high T_g , high resistance to chemicals, good dielectric and mechanical properties. Nevertheless, bio-based PIs were very limited, due to the difficult preparation of bio-based monomers as aromatic diamines cannot be prepared through biosynthesis. Thus, several bio-based diamine monomers were synthesized by chemical modification.^{23–29} For example, bio-based diamine monomers, 4,4'-diamino- α -truxillic acid dimethyl ester and 4,4'-diamino- α -truxillic acid diethyl ester, have been synthesized by photodimer of 4-aminocinnamic acid, a microorganism-derived aromatic monoamine.²⁶ The diamine monomer containing isosorbide structure has been successfully prepared by Mi and coworkers.²⁸ What's more, some bio-based difuranic diamines were prepared via the coupling reaction of furfurylamine with ketones or aldehydes.²⁹ However, these resulting partially bio-based PIs have been mainly synthesized using bio-based diamines containing aliphatic structures. There were few reports about bio-based fully aromatic PIs. Recently, Hu et al. have successfully incorporated

Additional Supporting Information may be found in the online version of this article.

© 2018 Wiley Periodicals, Inc.



SCHEME 1 Synthesis of diamines.

aromatic heterocyclic structure, adenine, in PI backbones, which resulted in the formation of bio-based fully aromatic PIs with high $T_g > 350$ °C and excellent mechanical properties.³⁰

Here, we report the synthesis of novel partially bio-based PIs derived from two new diamines with amide linkage, *N,N'*-bis(3-aminophenyl)furan-2,5-dicarboxamide (*m*-FDDA) and *N,N'*-bis(4-aminophenyl)furan-2,5-dicarboxamide (*p*-FDDA). The thermal properties, solubility, coefficient of thermal expansion (CTE), mechanical, and optical properties of these PIs are investigated. To compare with reported partially bio-based PIs, PIs derived from petrochemical-based monomer, isophthalic acid (IA), were also prepared and studied.

EXPERIMENTAL

Materials

3,3',4,4'-Biphenyltetracarboxylic dianhydride (BPDA) and 4,4'-(hexafluoroisopropylidene)diphthalic anhydride (6FDA) were purchased from Changzhou Sunlight Pharmaceutical Co. (Changzhou, China). 2,2-Bis[4-(3,4-dicarboxyphenoxy)phenyl] propane dianhydride (BPADA) was purchased from Shanghai Research Institute of Synthetic Resins (Shanghai, China). 2,5-Furandicarboxylic acid, 4-nitroaniline, 3-nitroaniline, thionyl chloride, pyridine, trimethylamine (Et₃N), isophthaloyl chloride, palladium on activated charcoal (10%Pd, Pd/C), hydrazinium hydrate solution (50%), and acetic anhydride were purchased from Aladdin Reagent (Shanghai, China). *N,N*-Dimethylacetamide (DMAc) was distilled from calcium hydride and stored over 4 Å molecular sieves. All other reagents for the study were commercially obtained and used as received without further purification. 2,5-Furandicarbonyl dichloride was prepared according to the method reported by Morales-Huerta et al.³¹ *N,N'*-Bis(4-aminophenyl)isophthalamide (*p*-IAPA) was prepared according to the method reported by Sarkar et al.³²

Measurements

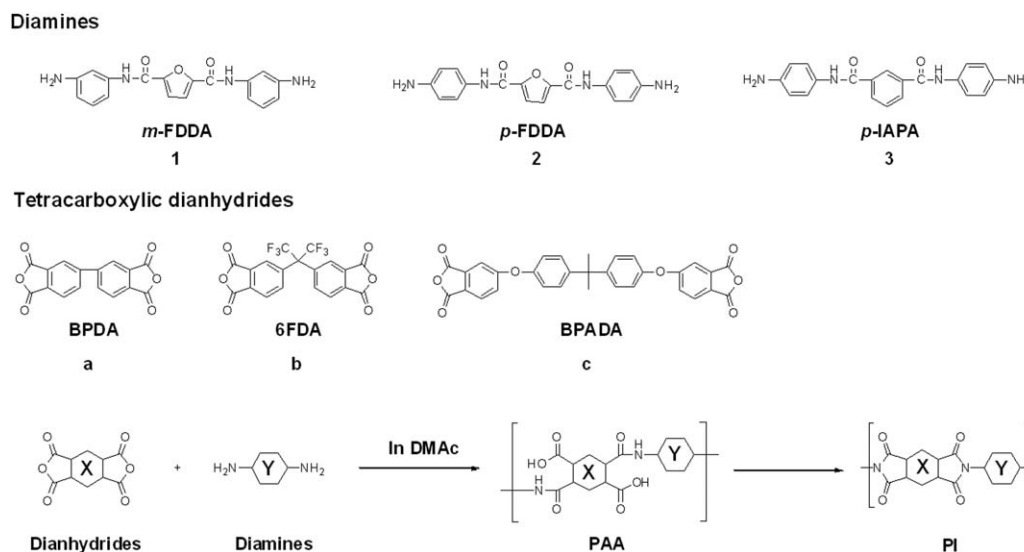
Fourier transform infrared (FT-IR) spectra of the powder samples were recorded with a Thermo Nicolet 6700 FT-IR spectrometer. All of the FT-IR spectra of the PI film samples were collected in the attenuated total reflection (ATR) mode with a 4-cm⁻¹ resolution for 128 scans each using a Cary 640 spectrometer (Agilent, Australia). Nuclear magnetic resonance (NMR) spectra were performed on a Bruker 400 AVANCE III spectrometer operating at 400 MHz for ¹H NMR

and 100 MHz for ¹³C NMR using dimethyl sulfoxide-*d*₆ (DMSO-*d*₆) as the solvent. Elemental analyses (C, H, N) were carried out on a Perkin-Elmer model 2400 II elemental analyzer. The inherent viscosities of the polymers were measured at 30 ± 0.1 °C with an Ubbelohde viscometer and the concentration was 0.5 g dL⁻¹ in DMAc. The melting point (MP) of the synthesized monomer was measured by micro MP apparatus. Thermogravimetric analyses (TGAs) of the PIs were performed on a Mettler Toledo-TGA/DSC I instrument to evaluate the thermal stability of the PIs at a heating rate of 10 °C min⁻¹ from 50 to 800 °C under nitrogen or air atmosphere (flow rate of 50 mL min⁻¹). The mechanical properties of the PI films such as tensile modulus, tensile strength, and elongation at break were measured and averaged on at least six film specimens by an Instron model 5567 tensile tester at room temperature. Ultraviolet-visible (UV-vis) spectra of the polymer films were recorded on a Lambda 950 UV/Vis/NIR Spectrophotometer. The wide-angle X-ray diffraction (WAXD) measurement of the PI films was undertaken on a Bruker D8 Advance with Cu Kα radiation (40 kV, 40 mA) at a scanning rate of 5° min⁻¹ from 5° to 50°. Thermo mechanical analysis (TMA) was performed by a METTLER TMA/SDTA841 at a heating rate of 10 °C min⁻¹. The CTE was recorded at the temperature range of 100–200 °C. Dynamic mechanical analysis (DMA) was carried out using a TA instrument DMA Q800 at a heating rate of 3 °C min⁻¹ and a load frequency of 1 Hz in film tension geometry. The storage modulus (*E'*) and the loss modulus (*E''*) were measured. T_g was determined as the peak temperature of tan δ curve. Differential scanning calorimetry (DSC) measurements of the PIs were performed on a Mettler Toledo-DSC I at a heating rate of 20 °C min⁻¹ under nitrogen atmosphere, and the temperature at the middle of the thermal transition was assigned as T_g .

Monomer Synthesis

N,N'-Bis(3-aminophenyl)furan-2,5-dicarboxamide (*m*-FDDA)

To a 500-mL three-necked round-bottom flask equipped with a dropping funnel were placed Et₃N (18.2142 g, 180.0 mmol) and 3-nitroaniline (24.8634 g, 180.0 mmol) in anhydrous DMAc (100 mL) and the mixture was magnetically stirred at room temperature for complete dissolution. Then, 2,5-furandicarbonyl dichloride (15.4384 g, 80 mmol) in DMAc (75 mL) was added dropwise to this solution under nitrogen atmosphere. After stirring at room temperature for 24 h, the mixture was trickled into water to afford a



SCHEME 2 Synthesis of PIs.

precipitate. The precipitate was collected by filtration, washed by water, and dried under vacuum at 95 °C to afford the crude dinitro product 24.7156 g, yield: 78%.

The dinitro compound (21.7115 g) was dissolved in DMAc (100 mL) and Pd/C (0.4515 g) was added as a catalyst. The hydrazinium hydrate solution (50%, 40 mL) was slowly dropped to the reaction mixture at 100 °C, and then stirred for 24 h under nitrogen atmosphere. Pd/C was removed by filtration and the filtrate was trickled into water to afford a precipitate. The crude product was recrystallized twice from methanol to obtain 15.4692 g white crystals, yield: 84%.

MP 239 °C. FT-IR (KBr, cm^{-1}): 1617 (C=O stretching), 3394 and 3332 (N—H stretching). ^1H NMR δ (400 MHz, $\text{DMSO}-d_6$, ppm): 9.99 (s, 2H), 7.33 (s, 2H), 7.02 (s, 2H), 7.00 (t, $J = 8.0$ Hz, 2H), 6.84 (d, $J = 8.0$ Hz, 2H), 6.36 (d, $J = 8.0$ Hz, 2H), 5.18 (s, 4H). ^{13}C NMR δ (100 MHz, $\text{DMSO}-d_6$, ppm): 155.7, 149.6, 148.7, 138.9, 129.6, 116.2, 110.9, 108.9, 106.7. Elemental analysis: found: C, 64.6; H, 4.9; N, 16.8%. Calc. for $\text{C}_{18}\text{H}_{16}\text{N}_4\text{O}_3$: C, 64.3; H, 4.8; N, 16.7%.

***N,N'*-Bis(4-aminophenyl)furan-2,5-dicarboxamide** (*p*-FDDA)

N,N'-Bis(4-aminophenyl)furan-2,5-dicarboxamide were prepared and characterized in a similar manner with *m*-FDDA to obtain product, yield: 80%. MP 139 °C. FT-IR (KBr, cm^{-1}): 1651 (C=O stretching), 3335 (N—H stretching). ^1H NMR δ (400 MHz, $\text{DMSO}-d_6$, ppm): 9.88 (s, 2H), 7.31 (d, $J = 8.7$ Hz, 4H), 7.25 (s, 2H), 6.57 (d, $J = 8.7$ Hz, 4H), 5.03 (s, 4H). ^{13}C NMR δ (100 MHz, $\text{DMSO}-d_6$, ppm): 155.5, 148.8, 146.4, 126.8, 123.2, 115.6, 114.3. Elemental analysis: found: C, 64.5; H, 4.8; N, 16.8%. Calc. for $\text{C}_{18}\text{H}_{16}\text{N}_4\text{O}_3$: C, 64.3; H, 4.8; N, 16.7%.

Polymer Synthesis and Film Preparation

Using two-step polycondensation via different methods [thermal imidization (H) and chemical imidization (C)], PIs (PIs)

were prepared from commercially available dianhydrides BPDA, 6FDA, and BPADA with diamines *m*-FDDA, *p*-FDDA, and *p*-IAPA (Scheme 2). The resulting PIs were referred to as PI-1-a to PI-3-c successively.

The poly(amic acid)s (PAAs, and PAA-2-b as an example) were synthesized by general synthetic route as follows: to a solution of diamine *p*-FDDA (1.6817 g, 4.0 mmol) in DMAc (15.6116 g), dianhydride 6FDA (2.2212 g, 4.0 mmol) was

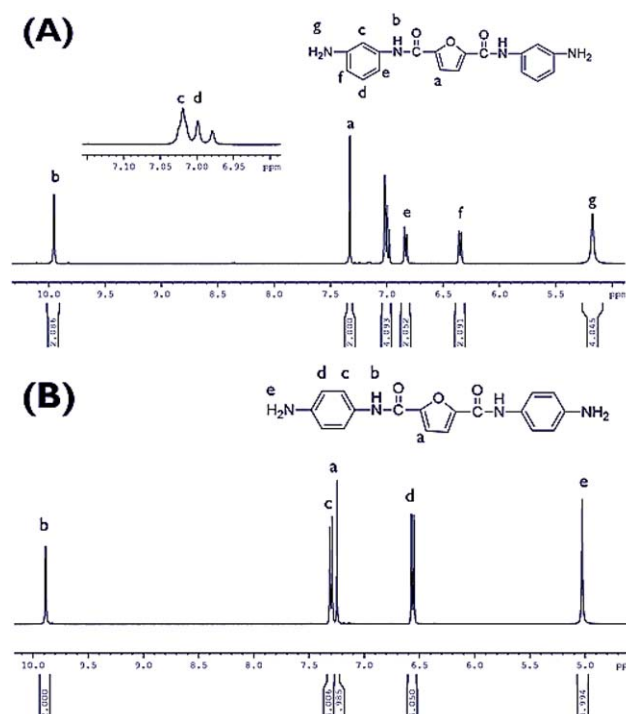


FIGURE 1 ^1H NMR spectrum of *m*-FDDA (A) and *p*-FDDA (B) in $\text{DMSO}-d_6$. [Color figure can be viewed at wileyonlinelibrary.com]

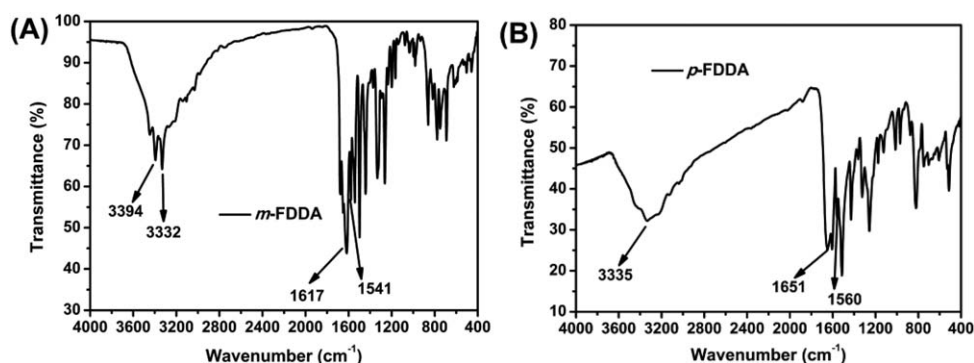


FIGURE 2 FT-IR spectra of *m*-FDDA (A) and *p*-FDDA (B).

added in one portion. The mixture was stirred in nitrogen at room temperature for 24 h to afford a viscous PAA solution with 20 wt% solid concentration. Then the resulting viscous PAA solution was diluted to 15 wt% with additional DMAc.

For the chemical imidization procedure, into the resulting PAA solution, the mixture of acetic anhydride/pyridine (2 mL/1 mL) was added. After stirring for 24 h, the solution was diluted with DMAc and slowly poured into a vigorously stirred ethanol. The precipitate was collected by filtration, and washed with hot ethanol and dried at 100 °C for 12 h. The solution of 10 wt% of resulting PI powder in DMAc was cast onto a clean glass substrate, placed in an oven at 80 °C overnight and then subjected to scheduled heating at 150 and 200 °C for 60 min at each temperature. The resulting PI films were obtained by immersing the glass plate in water followed by drying in an oven at 100 °C.

For the thermal imidization procedure, the PAA solution was cast onto a glass substrate and dried at 80 °C for 2 h in an air-convection oven to remove most of the solvent. The semi-dried PAA film was thermally converted to PI film by heating

at 150 and 280 °C for 60 min at each temperature under the air atmosphere. The resulting PI films were obtained by immersing the glass plate in water followed by dry in an oven at 100 °C.

PI-1-a: FT-IR (film, cm^{-1}): 1773 and 1707 ($\text{C}=\text{O}$ stretching, imide), 1655 ($\text{C}=\text{O}$ stretching, amide), 1354 ($\text{C}-\text{N}$ stretching).

PI-1-b: FT-IR (film, cm^{-1}): 1781 and 1716 ($\text{C}=\text{O}$ stretching, imide), 1673 ($\text{C}=\text{O}$ stretching, amide), 1362 ($\text{C}-\text{N}$ stretching). ^1H NMR δ (400 MHz, $\text{DMSO}-d_6$, ppm): 10.49 (s, 2H), 8.17 (d, $J = 7.8$ Hz, 2H), 7.94 (d, $J = 7.8$ Hz, 2H), 7.85 (s, 2H), 7.83 (d, $J = 8.7$ Hz, 2H), 7.75 (s, 2H), 7.55 (t, $J = 8.0$ Hz, 2H), 7.44 (s, 2H), 7.23 (d, $J = 7.8$ Hz, 2H).

PI-1-c: FT-IR (film, cm^{-1}): 1769 and 1714 ($\text{C}=\text{O}$ stretching, imide), 1671 ($\text{C}=\text{O}$ stretching, amide), 1356 ($\text{C}-\text{N}$ stretching).

PI-2-a: FT-IR (film, cm^{-1}): 1773 and 1706 ($\text{C}=\text{O}$ stretching, imide), 1661 ($\text{C}=\text{O}$ stretching, amide), 1362 ($\text{C}-\text{N}$ stretching).

TABLE 1 Thermal Properties and Inherent Viscosities of the PIs

PI	Bio-Based Content ^a (%)	Imidization	η_{inh}^b (dL g^{-1})	η_{inh}^c (dL g^{-1})	T_g^d (°C)	T_g^e (°C)	$T_{d5\%}^f$ (°C)		Char Yield ^g (%)	CTE ^h (ppm K^{-1})
							In N_2	In Air		
PI-1-a	17.6	H	0.49	—	334	— ⁱ	422	409	55	40.3
PI-1-b	16.2	C	0.97	0.64	329	290	437	412	50	42.4
PI-1-c	10.9	C	0.79	0.52	266	250	440	410	47	52.1
PI-2-a	17.6	H	0.81	—	350	— ⁱ	456	447	57	27.5
PI-2-b	16.2	C	1.14	0.72	364	— ⁱ	448	412	51	58.6
PI-2-c	10.9	C	0.74	0.49	287	— ⁱ	450	416	48	61.1
PI-3-c	0	C	1.21	0.89	283	— ⁱ	471	444	45	56.7

^a Calculated according to a method in the literature.³³

^b The inherent viscosities of PAAs were measured at a concentration of 0.5 g dL^{-1} in DMAc at 30 °C.

^c The inherent viscosities of PIs were measured at a concentration of 0.5 g dL^{-1} in DMAc at 30 °C.

^d T_g , as the peak temperature of $\tan \delta$ curve, was determined at a heating rate of 3 °C min^{-1} with DMA.

^e Obtained from DSC at a heating rate of 20 °C min^{-1} in N_2 .

^f Temperatures at which 5% weight loss were recorded by TGA at a heating rate of 10 °C min^{-1} .

^g Residual weight (%) when heated to 800 °C in nitrogen.

^h CTE was recorded from 100 to 200 °C at a heating rate of 10 °C min^{-1} by TMA.

ⁱ Not found.

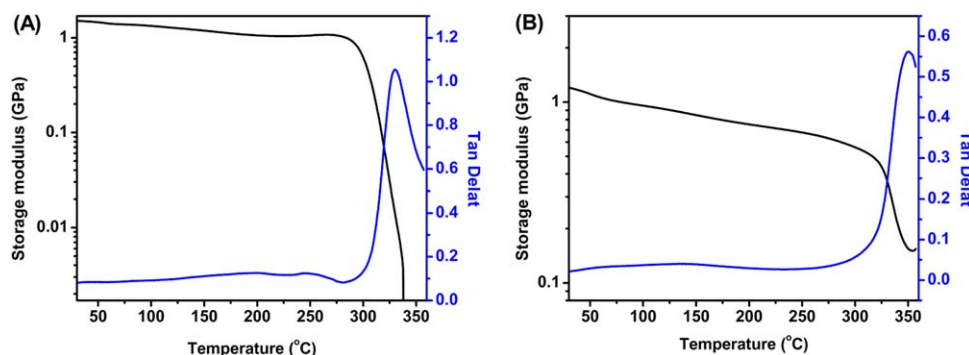


FIGURE 3 DMA curves of PIs: PI-1-a (A) and PI-2-a (B). [Color figure can be viewed at wileyonlinelibrary.com]

PI-2-b: FT-IR (film, cm^{-1}): 1781 and 1716 ($\text{C}=\text{O}$ stretching, imide), 1672 ($\text{C}=\text{O}$ stretching, amide), 1366 ($\text{C}-\text{N}$ stretching). ^1H NMR δ (400 MHz, $\text{DMSO}-d_6$, ppm): 10.50 (s, 2H), 8.18 (d, $J = 7.7$ Hz, 2H), 7.96 (d, $J = 7.7$ Hz, 2H), 7.89 (d, $J = 8.8$ Hz, 4H), 7.75 (s, 2H), 7.50 (s, 2H), 7.47 (d, $J = 8.0$ Hz, 4H).

PI-2-c: FT-IR (film, cm^{-1}): 1773 and 1709 ($\text{C}=\text{O}$ stretching, imide), 1672 ($\text{C}=\text{O}$ stretching, amide), 1362 ($\text{C}-\text{N}$ stretching).

PI-3-c: FT-IR (film, cm^{-1}): 1773 and 1709 ($\text{C}=\text{O}$ stretching, imide), 1673 ($\text{C}=\text{O}$ stretching, amide), 1368 ($\text{C}-\text{N}$ stretching). ^1H NMR δ (400 MHz, $\text{DMSO}-d_6$, ppm): 10.62 (s, 2H), 8.58 (s, 1H), 8.23–8.12 (m, 2H), 7.94 (d, $J = 7.7$ Hz, 6H), 7.78–7.66 (m, 1H), 7.48–7.30 (m, 12H), 7.14 (d, $J = 7.2$ Hz, 4H), 1.71 (s, 6H).

RESULTS AND DISCUSSION

Monomer Synthesis

The synthesis of two novel 2,5-FDCA-based diamines, *m*-FDDA and *p*-FDDA, is shown in Scheme 1. First, 2,5-furandicarboxyl dichloride³¹ was prepared from aromatic bio-based diacid, 2,5-FDCA, and then reacted with 3-nitroaniline/4-nitroaniline using Et_3N as HCl acceptor to afford dinitro intermediates. Finally, *m*-FDDA and *p*-FDDA were synthesized by hydrogenation of the corresponding dinitro intermediates in the presence of hydrazine hydrate and Pd/C. The

structures of *m*-FDDA and *p*-FDDA were confirmed by ^1H NMR, ^{13}C NMR (Supporting Information Figs. S1 and S2), and IR spectra. As shown in Figure 1, ^1H NMR spectra agree well with the chemical structures of diamines *m*-FDDA and *p*-FDDA. The amine protons (H_g for *m*-FDDA and H_e for *p*-FDDA) resonated in the region of 5.03–5.18 ppm, respectively. The furan protons (H_a) and amide protons (H_b) of *m*-FDDA resonated in the region of 7.33 and 9.99 ppm, respectively. The furan protons (H_a) and amide protons (H_b) of *p*-FDDA resonated in the region of 7.31 and 9.88 ppm, respectively. The FT-IR spectra of *m*-FDDA (A) and *p*-FDDA (B) are shown in Figure 2. In the FT-IR spectrum of *m*-FDDA and *p*-FDDA, the bands around 3332–3394 and 1617–1651 cm^{-1} , correspond to the N–H and $\text{C}=\text{O}$ stretching vibrations, respectively. The region at 1541–1560 cm^{-1} was assigned to the $\text{C}=\text{C}$ stretching vibration for furan rings. All of the spectroscopic data, obtained agreed with the expected structures.

Polymer Synthesis

Partially bio-based PIs were prepared from various aromatic dianhydrides with stoichiometric amounts of *m*-FDDA or *p*-FDDA via typical two-step methods [by thermal imidization (H) or chemical imidization (C)] (Scheme 2). Chemical imidization method was preferentially used except for PI-1-a and PI-2-a due to poor solubility of PIs in DMAc at room temperature. The inherent viscosities (η_{inh}) of PAAs and the corresponding PIs were in the range of 0.49–1.21 and 0.49–0.89 dL g^{-1} , respectively, which were summarized in Table 1.

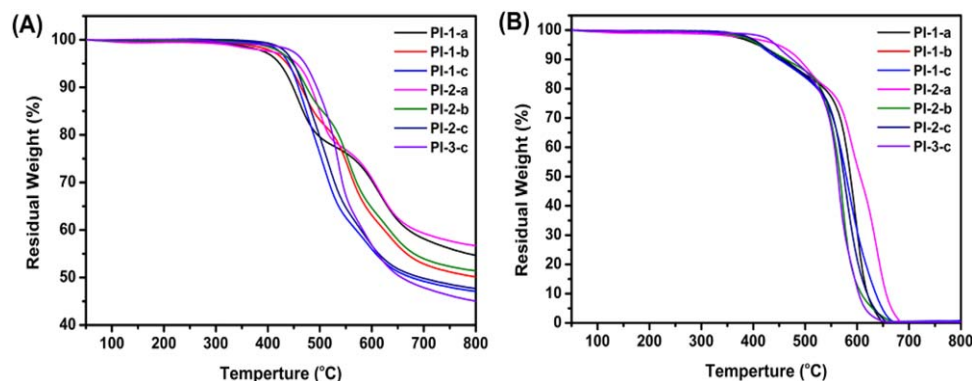


FIGURE 4 TGA curves of PIs in nitrogen (A) and air (B). [Color figure can be viewed at wileyonlinelibrary.com]

TABLE 2 Mechanical Properties of the PI Films

PI	Tensile Strength (MPa)	Tensile Modulus (GPa)	Elongation at Break (%)
PI-1-a	138	5.4	3.0
PI-1-b	95	2.9	5.3
PI-1-c	100	2.9	7.2
PI-2-a	120	4.0	12.3
PI-2-b	84	3.9	3.0
PI-2-c	79	2.5	8.7
PI-3-c	96	3.2	6.8

The high η_{inh} s of PIs were sufficient to cast tough and flexible films. According to US Department of Agriculture, the bio-based content of a resin is defined as the percentage of bio-based carbons in the total organic carbons of the resin.³³ The bio-based content of the 2,5-FDCA-based PIs in this study can be calculated according to this definition. The bio-based contents of 2,5-FDCA-based diamines, *m*-FDDA and *p*-FDDA, were 33.3%, whereas those of the dianhydrides were 0%. As summarized in Table 1, the bio-based contents of 2,5-FDCA-based PIs ranged from 10.9 to 17.6%.

The chemical structures of the PIs were characterized by ¹H NMR and FT-IR spectroscopy. The ¹H NMR spectra of representative PI-1-b and PI-2-b are shown in Supporting Information Figures S3 and S4, respectively. All of the signals have been assigned to the protons of the repeating unit. For PI-1-b and PI-2-b, the signals in the region of 7.44–7.51, 7.75–7.77, and 10.48–10.52 ppm were assigned to aromatic protons of dianhydride moiety (H_g), furan protons (H_a), and amide protons (H_b) in the PIs, respectively. The further assignment of the aromatic protons of PI-1-b and PI-2-b were confirmed by COSY spectra (Supporting Information Figs. S5 and S6).

The typical FT-IR spectra of PI-1-b and PI-2-b films are shown in Supporting Information Figure S7. The specific bands around 1781 cm⁻¹ (*asym* C=O stretching), 1716 cm⁻¹ (*sym* C=O

stretching), and 1362 cm⁻¹ (C–N stretching), affirming the imide ring formation, and the absorption band around 1673 cm⁻¹ originated due to C=O stretching vibration of amide.

Thermal Properties

The thermal properties of the PIs are evaluated by DMA, DSC, TGA, and TMA. The thermomechanical properties of PI-1-a and PI-2-a were analyzed via DMA in Figure 3. The storage moduli (E') of PI-1-a and PI-2-a were 1.20 and 1.51 GPa, respectively. Moreover, the storage modulus (E') of the PIs as function of temperatures decreased with reducing stiffness. The T_g values of 334 and 350 °C were observed, as defined by the peak temperature in $\tan \delta$ curves, which were higher than those measured by DSC. As listed in Table 1, all PIs characterized by DMA showed high T_g values above 260 °C, which were correlated with rigidity and conformation of the polymer backbones. Such T_g s of partially bio-based PIs are much higher than the T_g s of reported PIs containing 2,5-furan moiety, which were about 116–143 °C, due to the fully aromatic structure.²⁹ The *p*-FDDA-based PI series (PI-2) possessed obviously higher T_g values than those of the corresponding counterpart *m*-FDDA-based PI series (PI-1) with *m*-phenylene substitution in diamine moiety, which was resulted from the linear and stiff backbone structure of *p*-FDDA-based PI series. The PI-1-a with rigid dianhydride BPDA showed high T_g value of 334 °C, while PI-1-c with flexible dianhydride BPADA exhibited low T_g value of 266 °C. Interestingly, PI-3-c based on *p*-IAPA with higher η_{inh} value exhibited slightly lower T_g compared with PI-2-c derived from *p*-FDDA. It was probably due to the formation of more rigid and planar conformation of 2,5-FDCA-based PI, which was expected to offer higher T_g value compared with PI-3-c.³⁴ Additionally, DSC curves of the PIs are also tested and shown in Supporting Information Figure S8. However, the T_g of most PIs were not obvious due to low sensitivity of DSC test of PI resin with rigid molecular structure.

The thermal stability of the PIs was evaluated by TGA as shown in Figure 4. The temperature of 5% weight loss

TABLE 3 Solubility of the PIs^a

PI	Solvents ^b					
	<i>m</i> -Cresol	DMAc	NMP	DMSO	Acetone	THF
PI-1-a	++	+	+	+-	—	—
PI-1-b	++	++	++	++	—	—
PI-1-c	++	++	++	+	—	—
PI-2-a	—	—	—	—	—	—
PI-2-b	++	++	++	++	—	—
PI-2-c	++	++	++	+	—	—
PI-3-c	++	++	++	++	—	—

^a The qualitative solubility was tested with 10 mg samples in 1 mL of solvent. ++: soluble at room temperature; +: soluble on heating; +-: partially soluble on heating; -: insoluble on heating.

^b DMAc: *N,N*-dimethylacetamide; NMP: *N*-methyl-2-pyrrolidone; DMSO: dimethyl sulfoxide; THF: tetrahydrofuran.

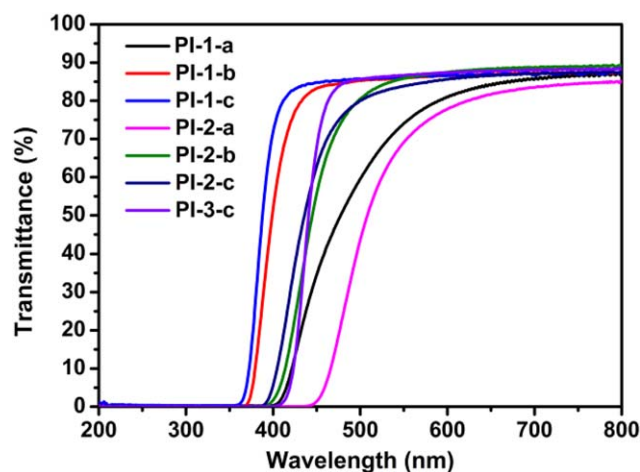


FIGURE 5 UV-vis spectra of PI films. [Color figure can be viewed at wileyonlinelibrary.com]

($T_{d5\%}$) in nitrogen and air atmospheres exceeded 400 °C, which suggested good thermal stability of 2,5-FDCA-based PIs. *p*-FDCA-based PI series (PI-2) exhibited slightly higher $T_{d5\%}$ than those of *m*-FDCA-based PI series (PI-1) due to their rigid backbones. What's more, PI-2-c showed a decrease in $T_{d5\%}$ compared with the PI-3-c, which suggested the relatively lower thermal stability of furan moiety compared with benzene moiety. The excellent thermal properties of 2,5-FDCA-based PIs were attributed to fully aromatic structures compared with other analogous bio-based PIs containing aliphatic structures.^{25–29}

The CTE values of 2,5-FDCA-based PIs are also summarized in Table 1, which were in the range of 27.5–61.1 ppm K^{−1}. The CTE value generally increased due to the flexible linkage in aromatic dianhydride moiety (CTE value: BPDA < 6FDA < BPADA). The PI-2-a exhibited the lowest CTE value (27.5 ppm K^{−1}) among the PIs due to its relatively rod-like backbone structure, causing a drastic chain alignment toward the direction parallel to the film plane. The CTE value of PI-3-c is lower than PI-2-c, probably owing to increasing intermolecular hydrogen bonds.³⁵

TABLE 4 Optical Properties of the PI Films

PI	d^a (μm)	λ_0^b (nm)	T_{400}^c (%)	T_{450}^c (%)	T_{500}^c (%)
PI-1-a	30	397	0	35	60
PI-1-b	26	368	52	83	85
PI-1-c	24	362	72	85	86
PI-2-a	32	437	0	1	44
PI-2-b	28	389	2	56	80
PI-2-c	20	385	6	63	80
PI-3-c	23	400	0	68	86

^a Film thickness.

^b UV cut-off wavelength.

^c Transmittance at 400, 450, and 500 nm, respectively.

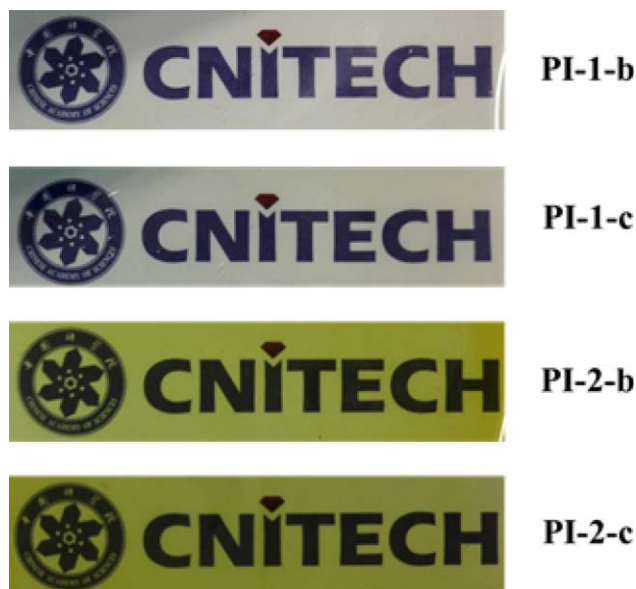


FIGURE 6 Photographs of the PI films. [Color figure can be viewed at wileyonlinelibrary.com]

Mechanical Properties

The mechanical properties of the PI films are listed in Table 2. The partially bio-based PI films exhibited good mechanical properties with tensile strengths of 79–138 MPa, tensile moduli of 2.5–5.4 GPa, and elongations at break of 3.0–12.3%. Among these PI films, the tensile strength and tensile modulus of PI-1-a and PI-2-a were more than 120 MPa and 4.0 GPa, respectively, which were attributed to rigid structure of BPDA dianhydride. It is noted that the tensile strength and tensile modulus of PI-3-c were about 96 MPa and 3.2 GPa, which were higher than those of PI-2-c (79 MPa and 2.5 GPa). Such comparison suggested that the negative effect of furan rings on intermolecular hydrogen bonding between amide groups has weakened mechanical properties of PIs.³⁶

Solubility

The solubility of the PIs was tested qualitatively in various organic solvents, and the results are shown in Table 3. It was found that the PI-1-b, PI-2-b, PI-1-c, and PI-2-c showed better solubility than PI-1-a and PI-2-a in common organic solvents such as *m*-cresol, NMP, and DMAc, owing to flexible connecting structure disturbing chain packing and reduced the inter-chain interaction to enhance solubility. Furthermore, the PI-1-a containing *m*-phenylene substitution exhibited better solubility compared with PI-2-a.

Optical Properties

The UV-visible spectra of some representative PI films are illustrated in Figure 5, and the cut-off wavelength (absorption edge, λ_0) and the transmittance at 400, 450, and 500 nm from these spectra are listed in Table 4. All partially bio-based films show the λ_0 at 437–362 nm. The transmittances of PI-1 series with *m*-phenylene substitution in

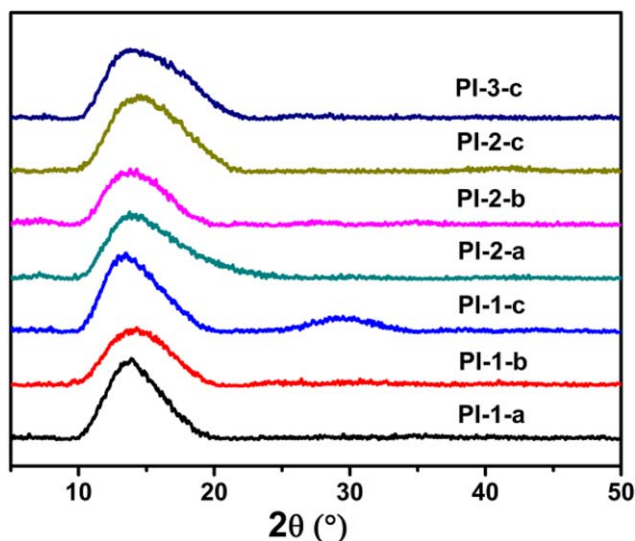


FIGURE 7 WAXD of the PI films. [Color figure can be viewed at wileyonlinelibrary.com]

diamine moiety measured at 450 nm are significantly higher than those of corresponding PI-2 series. The fairly transparent and almost colorless films of PI-1 series are shown in Figure 6. PI-1-a and PI-2-a possess poor transparency, probably due to oxidation of thermally less stable terminal amino groups in thermal imidization and high electron affinity of BPDA dianhydride moiety which enhanced inter- and intramolecular charge transfer interactions.³⁷ Furthermore, the petroleum-based PI-3-c showed similar transparency with partially bio-based PI-2-c.

X-Ray Diffraction

The crystallinity of the PI films was characterized by WAXD. The WAXD patterns of all the films were broad without obvious peak features, which indicated that they were all amorphous (Fig. 7). The petroleum-based PI-3-c showed the similar amorphous nature with 2,5-FDCA-based PI-2-c.

CONCLUSIONS

In this study, we report the successful synthesis of two series of novel partially bio-based PIs from two 2,5-FDCA-based diamines, *N,N'*-bis(3-aminophenyl)furan-2,5-dicarboxamide (*m*-FDDA), and *N,N'*-bis(4-aminophenyl)furan-2,5-dicarboxamide (*p*-FDDA) via conventional two-step method. The PIs showed high T_g up to 364 °C, $T_{d5\%}$ up to 456 °C, and excellent mechanical properties with tensile strengths of 79–138 MPa, tensile moduli of 2.5–5.4 GPa, and elongations at break of 3.0–12.3%. The more rigid planar conformation by the introduction of furan in polymer resulted in higher T_g of PIs. PIs with *m*-phenylene substitution exhibited higher optical transparency and solubility. The resulting PI films may be promising bio-based materials, which can be used in the application of optoelectronic and microelectronic devices.

ACKNOWLEDGMENTS

This work was supported by National Natural Science Foundation of China (grant no. 51403225), Science and Technology Planning Project of Guangdong Province, China (no: 2016B090906004), Scientific research Plan Project of the State Administration of Quality Supervision, Inspection and Quarantine (no. 2017IK255), and the program for Ningbo Municipal Science and Technology Innovative Research Team (grant no. 2016B10005 and 2015B11002).

REFERENCES AND NOTES

- 1 C. Vilela, A. F. Sousa, A. C. Fonseca, A. C. Serra, J. F. J. Coelho, C. S. R. Freire, A. J. D. Silvestre, *Polym. Chem.* **2014**, *5*, 3119.
- 2 D. Dakshinamoorthy, S. P. Lewis, M. P. Cavazza, A. M. Hoover, D. F. Iwig, K. Damodaran, R. T. Mathers, *Green Chem.* **2014**, *16*, 1774.
- 3 A. Noreen, K. M. Zia, M. Zuber, S. Tabasum, A. F. Zahoor, *Prog. Org. Coat.* **2016**, *91*, 25.
- 4 H. Zhang, M. W. Grinstaff, *Macromol. Rapid Commun.* **2014**, *35*, 1906.
- 5 A. P. Gupta, V. Kumar, *Eur. Polym. J.* **2007**, *43*, 4053.
- 6 G.-Y. A. Tan, C.-L. Chen, L. Li, L. Ge, L. Wang, I. M. N. Razaad, Y. Li, L. Zhao, Y. Mo, J.-Y. Wang, *Polymers* **2014**, *6*, 706.
- 7 A. Gandini, T. M. Lacerda, *Progr. Polym. Sci.* **2015**, *48*, 1.
- 8 C. Voirin, S. Caillol, N. V. Sadavarte, B. V. Tawade, B. Boutevin, P. P. Wadgaonkar, *Polym. Chem.* **2014**, *5*, 3142.
- 9 C. Zhang, T. F. Garrison, S. A. Madbouly, M. R. Kessler, *Progr. Polym. Sci.* **2017**, *71*, 91.
- 10 A. Gandini, T. M. Lacerda, A. J. F. Carvalho, E. Trovatti, *Chem. Rev.* **2016**, *116*, 1637.
- 11 S. Laurichesse, L. Avérous, *Progr. Polym. Sci.* **2014**, *39*, 1266.
- 12 M. Gomes, A. Gandini, A. J. D. Silvestre, B. Reis, *J. Polym. Sci. Part A: Polym. Chem.* **2011**, *49*, 3759.
- 13 M. Jiang, Q. Liu, Q. Zhang, C. Ye, G. Zhou, *J. Polym. Sci. Part A: Polym. Chem.* **2012**, *50*, 1026.
- 14 V. Tsanakis, G. Z. Papageorgiou, D. N. Bikiaris, *J. Polym. Sci. Part A: Polym. Chem.* **2015**, *53*, 2617.
- 15 Y. Jiang, D. Maniar, A. J. J. Woortman, G. O. R. A. van Ekenstein, K. Loos, *Biomacromolecules* **2015**, *16*, 3674.
- 16 J.-H. Wu, W.-C. Chen, G.-S. Liou, *Polym. Chem.* **2016**, *7*, 1569.
- 17 T. Higashihara, M. Ueda, *Macromolecules* **2015**, *48*, 1915.
- 18 P. M. Budd, N. B. McKeown, *Polym. Chem.* **2010**, *1*, 63.
- 19 X. Xiao, X. Qiu, D. Kong, W. Zhang, Y. Liu, J. Leng, *Soft Matter* **2016**, *12*, 2894.
- 20 X. Xiao, D. Kong, X. Qiu, W. Zhang, F. Zhang, L. Liu, Y. Liu, S. Zhang, Y. Hu, J. Leng, *Macromolecules* **2015**, *48*, 3582.
- 21 C.-L. Tsai, G.-S. Liou, *Chem. Commun.* **2015**, *51*, 13523.
- 22 C.-L. Tsai, T.-M. Lee, G.-S. Liou, *Polym. Chem.* **2016**, *7*, 4873.
- 23 X. Ji, Z. Wang, J. Yan, Z. Wang, *Polymer* **2015**, *74*, 38.
- 24 A. Kumar, S. Tateyama, K. Yasaki, M. A. Ali, N. Takaya, R. Singh, T. Kaneko, *Polymer* **2016**, *83*, 182.
- 25 S. S. Kuhire, P. Sharma, S. Chakrabarty, P. P. Wadgaonkar, *J. Polym. Sci. Part A: Polym. Chem.* **2017**, *55*, 3636.
- 26 P. Suvannasara, S. Tateyama, A. Miyasato, K. Matsumura, T. Shimoda, T. Ito, Y. Yamagata, T. Fujita, N. Takaya, T. Kaneko, *Macromolecules* **2014**, *47*, 1586.

- 27** G. Yang, R. Zhang, H. Huang, L. Liu, L. Wang, Y. Chen, *RSC Adv.* **2015**, *5*, 67574.
- 28** Z. Mi, Z. Liu, C. Tian, X. Zhao, H. Zhou, D. Wang, C. Chen, *J. Polym. Sci. Part A: Polym. Chem.* **2017**, *55*, 3253.
- 29** L. B. Maktouf, I. Ghorbel, A. Afli, S. Abid, A. Gandini, *Polym. Bullet.* **2011**, *67*, 1111.
- 30** J. Hu, Z. Wang, Z. Lu, C. Chen, M. Shi, J. Wang, E. Zhao, K. Zeng, G. Yang, *Polymer* **2017**, *119*, 59.
- 31** J. Carlos Morales-Huerta, A. Martínez de Ilarduya, S. Muñoz-Guerra, *Polymer* **2016**, *87*, 148.
- 32** A. Sarkar, A. S. More, P. P. Wadgaonkar, G. J. Shin, J. C. Jung, *J. Appl. Polym. Sci.* **2007**, *105*, 1793.
- 33** G. A. Norton, S. L. Devlin, *Biores. Technol.* **2006**, *97*, 2084.
- 34** I.-C. Yeh, B. C. Rinderspacher, J. W. Andzelm, L. T. Cureton, J. L. Scala, *Polymer* **2014**, *55*, 166.
- 35** C. H. R. M. Wilsens, Y. S. Deshmukh, B. A. J. Noordover, S. Rastogi, *Macromolecules* **2014**, *47*, 6196.
- 36** K. Luo, Y. Wang, J. Yu, J. Zhu, Z. Hu, *RSC Adv.* **2016**, *6*, 87013.
- 37** C.-P. Yang, Y.-Y. Su, *Polymer* **2005**, *46*, 5797.